

Chapter 6

Dynamic Coupling Between Respiratory and Cardiovascular System

Federica Censi, Giovanni Calcagnini, and Sergio Cerutti



Abstract The analysis of non-linear dynamics of the coupling among interacting quantities can be very useful for understanding the cardiorespiratory and cardiovascular control mechanisms. In this chapter RP is used to detect and quantify the degree of non-linear coupling between respiration and spontaneous rhythms of both heart rate and blood pressure variability signals. RQA turned out to be suitable for a quantitative evaluation of the observed coupling patterns among rhythms, both in simulated and real data, providing different degrees of coupling. The results from the simulated data showed that the increased degree of coupling between the signals was marked by the increase of PR and PD, and by the decrease of ER. When the RQA was applied to experimental data, PD and ER turned out to be the most significant variables, compared to PR. A remarkable finding is the detection of transient 1:2 PL episodes between respiration and cardiovascular variability signals. This phenomenon can be associated to a sub-harmonic synchronization between the two main rhythms of HR and BP variability series.

F. Censi (✉) • G. Calcagnini
Italian National Institute of Health, Viale Regina Elena 299, 00161 Roma, Italy
e-mail: federica.censi@iss.it; giovanni.calcagnini@iss.it

S. Cerutti
Polytechnic University of Milan, Piazza Leonardo da Vinci 32, 20133 Milano, Italy
e-mail: sergio.cerutti@polimi.it

6.1 Introduction

Physiological rhythms are central to life: complex or simple rhythms usher the activities of living systems, involving several phenomena such as locomotion, metabolism, and hormonal regulation. Some rhythms are maintained throughout life, and even a brief interruption leads to death. Other rhythms may be expression of pathological conditions and thus indicate an unpaired equilibrium. Oscillating phenomena in living systems range within a wide frequency band, from firing rates of nervous fibers to circadian oscillations up to monthly hormonal changes. The study of biological oscillations is important for a reliable comprehension of the living system organization and functioning. The rhythms interact with one another and with the external environment. The analysis of the genesis of a biological rhythm and the interpretation of the conditions which change its temporal and morphological features allow to advance hypotheses on the mechanisms underlying several living processes. In addition, variations of rhythms and/or of their interaction outside normal limits, or appearance of new rhythms and coupling conditions where none existed previously, are associated with malfunctioning, disease, transient or permanent pathological states. An understanding of the mechanisms of physiological rhythms requires an approach that integrates mathematics and physiology.

Cardiovascular variables are characterized by oscillations even in stationary physiological conditions. In the range 0.03–0.4 Hz, such oscillations reflect complex control mechanisms mediated by the autonomic nervous system (ANS). Over the last 20 years a great deal of research regarding short-term heart rate and blood pressure variability has been carried out using linear and non-linear approaches.

Although both approaches for the analysis of the heart rate variability provide important pieces of information about the ANS, other physiological variables as well as external stimuli are involved in the autonomic nervous system control mechanisms. The interactions between respiration, heart rate and blood pressure fluctuations, which reflect the cardiovascular and cardiorespiratory couplings, are considered to be of paramount importance for the study of the functional organization of the ANS. The cardiovascular control is performed by a number of mechanisms and pathways which simultaneously act in either synergic or antagonistic manner. Feedback control loops mediated by baroreceptors, chemoreceptors or mechanoreceptors activity regulate blood pressure, heart rate and respiratory dynamics; oscillators located in the brain stem and in the heart modify respiration and vasomotion; local peripheral oscillators control microvascular resistances and flows. When responding to the needing of an organism the interactions among these oscillator can provoke prevalence of one or more oscillating structures on the others, and/or synchronization phenomena.

The analysis of non-linear dynamics of the coupling among interacting quantities turned out to be more adequate for understanding the cardiorespiratory and cardiovascular couplings than traditional linear methods [1–5]. Several non-linear techniques have been applied to cardiorespiratory data in order to analyze their coupling mechanisms [6–8].

The recurrence plot analysis was introduced by Eckmann et al. [9] in physics as a graphical method designed to locate recurrent and intermittent patterns in experimental time series. This technique was then enhanced by the introduction of several variables to quantify the recurrence plot features [10], which turn out to be useful in assessing transient behavior of experimental data sets in different scientific explorations [11–18].

The recurrence plots were first introduced to analyze the regularity of single time series. According to this traditional approach a recurrence plot (RP) is a graphical tool which can be used to observe whether recurrences characterize the dynamics of a given system. After the introduction of the recurrence map to analyze single time series, Porta et al. [19] suggested the use of this tool to analyze the interaction among signals. Nowadays, the approaches to study the interaction among different time series by using the recurrence map, are the recurrence, the cross-recurrence and the joint recurrence plot analysis [20, 21]. The first merely compares the periodicity of two (or more) time series, without employing the time embedding procedure [19, 22, 23], and it could be considered a sort of multivariate RP; the other approaches are somewhat more complex and quantify the recurrences in a distance matrix between the two embedded series.

In this chapter RP will be used to detect and quantify the degree of non-linear coupling between respiration and spontaneous rhythms of both heart rate and blood pressure variability signals. The analysis could of course be extended by evaluating the recurrence of the three signals together, but this approach would render the clinical interpretation of the results much more difficult.

6.2 Recurrence Plot Analysis for the Interaction Between Two Series

The interactions among rhythms causing frequency and/or phase synchronization represent a particular class of non-linear phenomena. Two interacting oscillators are N:M phase locked (PL) if marked events of one oscillator occur at fixed phases of the other oscillator. For this particular interaction, the spectral coherence (linear method) is often found not to be significant (but for a 1:1 coupling), since no phase synchronization or weak correlation between amplitudes are present. The notion of phase synchronization, which is often referred to as entrainment or phase locking, has been extensively used for analyzing and modeling interaction between different physiological sub-systems. Entrainment phenomena, arising from periodic stimulation of non-linear oscillators, have been studied in a number of biomedical applications [24–26]. Particularly, a number of studies focused on the synchronization between heartbeat or heart rate fluctuations and respiratory rhythm [27–30].

In 1994, Porta et al. [19] first suggested the use of the RP to measure synchronization among signals and to analyze the interactions between two or more signals.

Following this approach, in a bidimensional case (time series $x(t)$ and $y(t)$) RP is a representation of the normalized distance between the points $[x(i), y(i)]$ and $[x(j), y(j)]$, plotted in the time-to-time domain (i, j) . The time series “belong” to different systems: time series $x(t)$ is a measurement from system X and y is the measurement of the system Y.

The normalized distance $D(i, j)$ is computed as follows:

$$D(i, j) = \sqrt{\frac{[x(i) - x(j)]^2}{\text{var}(x)} + \frac{[y(i) - y(j)]^2}{\text{var}(y)}} \quad (6.1)$$

where $\text{var}(\cdot)$ indicates the time series variance. If the two points are sufficiently close to each other, i.e. the distance $D(i, j)$ is lower than a fixed cut-off value, a dot is plotted in (i, j) . A recurrent point in (i, j) means that the interaction between the signals in the instant i is almost the same as in the instant j , i.e. the interaction is recurring. If $D(i, j)$ is higher than the threshold, (i, j) is a not recurrent point.

The distance threshold is usually set to as a percentage of the maximum distance value, computed as the 95th percentile [10]. Since the distance between a point and itself is zero ($D(i, i) = 0$), the main diagonal line in the plot is always visible. Moreover the plot is symmetric, since $D(i, j) = D(j, i)$ according to the definition of distance given in (6.1).

A recurrent point indicates an isolated recurrence of an amplitude relationship between the signals. Line segments parallel to the main diagonal come from points close to each other successively forward in time $((i, j), (i + 1, j + 1), \dots, (i + T, j + T))$. Thus, a recurrent diagonal line indicates a stable recurrence of the relationship for a time interval corresponding to the length of the diagonal (T). The time interval separating adjacent diagonals is the recurrence period. Recurrent points organized in rows and columns do not convey any information about the timing of the periodicity, since they are not successively forward in time.

6.2.1 Application to Test Data Set

Figure 6.1 makes it clear how a RP can detect recurrent structures on a test data set. In this figure the RP of the x - and the z -components of the Lorentz system is shown (lower panel), together with the time courses of the two variables (upper panel). In the RP, the isolated recurrent points are plotted in gray while those organized in diagonal lines are in black.

Four sections have been selected, in the plot, each showing a different kind of coupling. In section I the RP features diagonal segments recurring without temporal periodicity, indicating that there exist non-periodical intervals of synchronization (i.e. the signals show a stable phase relationship). Such a periodicity is instead present in section III, where diagonal lines are separated by the same time intervals (recurrent period). In section II and IV both signal amplitudes are close to zero and

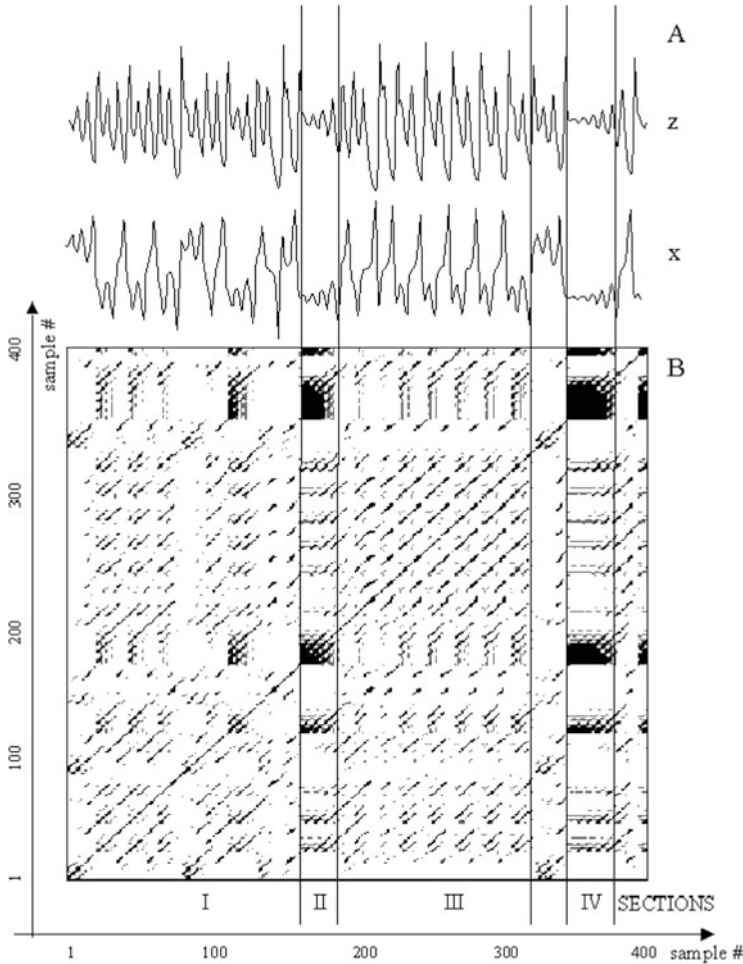


Fig. 6.1 Trackings of the x - and z -component of the Lorenz system (panel A) and the recurrence plot associated (panel B), with the isolated recurrent points in gray and those forming diagonal lines in black. The vertical lines indicate four sections, each showing a different kind of coupling between the two series. The values of the RPQ variables for the overall recurrence plot are: $PD = 65.2\%$, $PR = 15.1\%$, $ER = 2.9$

recurrent points in the map are organized not only in diagonals but also in rows and columns. In fact all points within these two sections are recurrent with each other and not only with those successively forward in time.

Figure 6.2 shows the deterministic structure of a 1:1 Phase locking (PL) phenomena (panels A and B), with diagonals recurring every period. RP of a 1:2 phase locking (panel D) shows diagonal lines recurring every period of the slower oscillator (series 2, panel B), and isolated points recurring each period of the faster one (series 1, panel A).

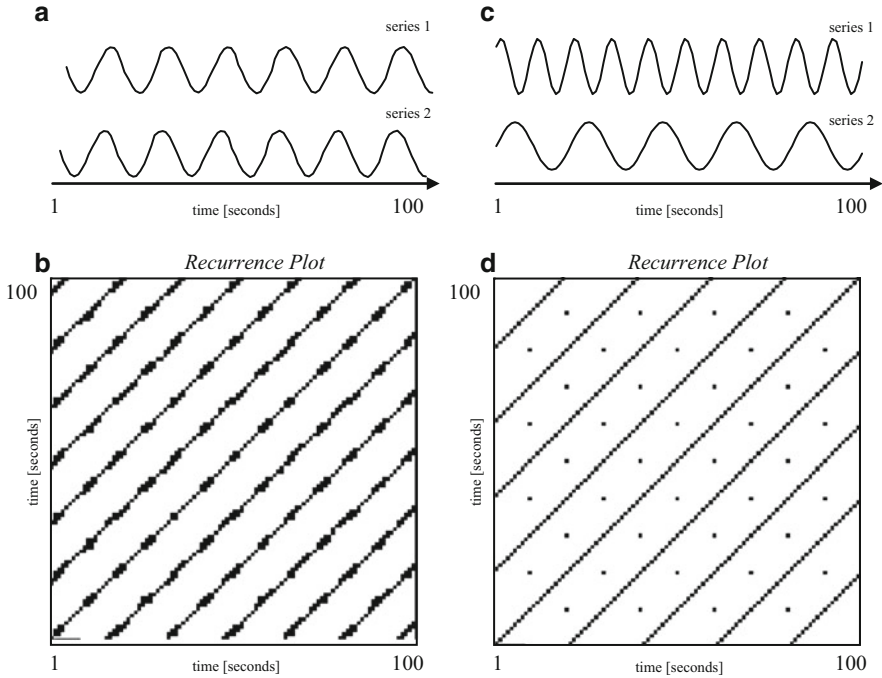


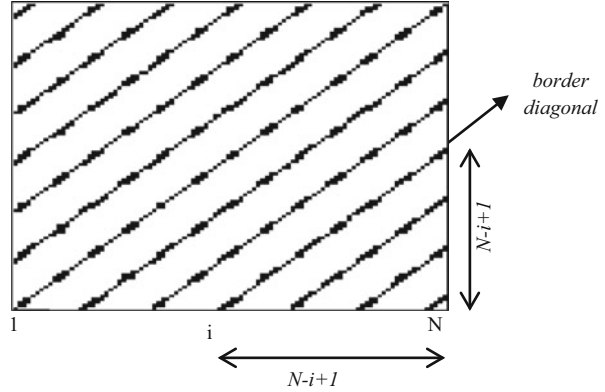
Fig. 6.2 Example of RP for a PL 1:1 and PL 1:2 (panels **B** and **D** respectively) between the two series shown in panels **A** and **C**, respectively

6.2.2 Quantification

Although these plots can provide a qualitative assessment of the system, as recurrent points and diagonals increase, the visual inspection is not easy. Thus, there is the need to quantify the organization of recurrence points into specific patterns.

Three descriptors of the RP plot features are commonly used [10]. One is the percentage of plot occupied by recurrent points, namely Percent Recurrence (PR), defined as the percent ratio between the number of recurrent points and the total number of all possible points. It quantifies the number of time instants characterized by a recurrence in the signals interaction: the more frequent the signal dynamics, the higher the PR value. Another descriptor is the percentage of recurrent points forming diagonal lines called Percent Determinism (PD), defined as the percent ratio between the number of recurrent points forming diagonals longer than a fixed threshold (l) and the total number of recurrent points. This variable discriminates between the isolated recurrent points and those forming diagonals. Since a diagonal represents points close to each other successively forward in time, PD also contains the information about the duration of a stable interaction: the longer the interactions, the higher the PD value. A third variable is the Entropy of Recurrence (ER), which is the Shannon entropy of diagonal length distribution, defined as follows:

Fig. 6.3 Border diagonals in the RP



$$ER = - \sum_{L=2}^N p_L \log_2 p_L \quad (6.2)$$

p_L is the probability that a diagonal is L -point long, with L ranging from the chosen threshold l to the main diagonal length (which correspond to the total number of points of the analyzed time series, i.e. N). p_L is defined as the ratio between the number of L -point long diagonals, and the total number of diagonals. ER is measured in bits of information, because of the base-2 logarithm in Eq. (6.2). Thus, whereas PD accounts for the number of the diagonals, ER quantifies the distribution of the diagonal line lengths. The more different the lengths of the diagonals, the more complex the deterministic structure of the RP.

A more complex dynamics will require a larger number of bits (ER) to be represented than a deterministic dynamics such as a 1:1 phase locking phenomena reported in Fig. 6.2, panels A and B. However the estimation of the ER on the basis of Eq. (6.2) may lead to its over-estimation since in 1:1 phase locking for example, the diagonal lengths are different because of a border effect and not because of the recurrence end. A diagonal starting from position $(i, 1)$ and ending at position $(N, N - i + 1)$ is called a border diagonal (Fig. 6.3). A border diagonal is long $N - i + 1$ points. Of course, the distribution of the border diagonals leads to a misleading (over-) estimation of the ER , since for the deterministic 1:1 phase locking pattern shown in Fig. 6.2 (panels A and B), six border diagonals with different lengths are detectable.

In order to avoid the border effect, a corrected diagonal length (CDL) has been introduced in such a way that a border diagonal is considered to be long as much as the main diagonal (N samples). In particular the correction has been applied to all L -long border diagonals (with $L > l$) according to the following formula:

$$CDL = L \frac{N}{N - i + 1} \quad (6.3)$$

Unfortunately, also the number of diagonals may affect the estimation of ER. When the diagonal are a few, ER has a relatively low value, regardless the lengths of the diagonal. In order to take into account the number of diagonals, ER has been divided by the ratio between the number of recurrent points forming diagonals and the total number of recurrent points. This ratio (which is the not-percent PD) varies between 0 and 1, in such a way that if the number of diagonals increases ER decreases and vice versa.

The choice of the threshold value l for the length of the diagonals is crucial for the correct estimation of both PD and ER. The threshold l should be chosen according to the frequency content of the analyzed time series: high values for l lead to the under-estimation of PD and ER, while low values to their over-estimation. The choice of l value implies the definition of the minimum duration of a stable recurrence. A recurrence is considered stable if it lasts at least half period of the faster oscillator. This choice allows the classification of various coupling phenomena, either simulated or experimentally observed, as showed in the following paragraphs.

6.3 Quantification of Recurrences of the Van Der Pol Model

In order to test how the RPs descriptors work, we used the Van Der Pol model. It is described by the following non-linear differential second order equation:

$$\ddot{x} + \varepsilon (x^2 - 1) \dot{x} + \omega_0^2 x = f(t) \quad (6.4)$$

$f(t)$ is the forcing term, and ε is a model parameter (it must be a positive constant). In the absence of forcing term the Van der Pol oscillator exhibits periodic oscillations at ω_0 , sustained by the non-linear term. When $f(t)$ is a periodic term, different kinds of interference occur between the forcing term $f(t)$ and the Van Der Pol oscillator $x(t)$, by varying the amplitude and frequency of the external stimulus. Although this model is not strictly interpretable from a physiological point of view, it well reproduces interaction phenomena observed in experimental data, such as sub-harmonic synchronization and full entrainment.

By varying the amplitude and the frequency of the sinusoidal forcing term $f(t)$, we analyzed three coupling patterns between the forcing term and the Van der Pol oscillator: no interaction, sub-harmonic synchronization, and full entrainment (Fig. 6.4, upper part, panels A–C, respectively). Sub-harmonic synchronization can be obtained by setting the frequency of the sinusoidal forcing term close to twice ω_0 (self-oscillations). Full-entrainment was obtained by applying a forcing term with a relatively high amplitude.

Figure 6.4 shows the RPs and the RQA results for each analyzed coupling pattern (middle part). The degrees of coupling of the three analyzed phenomena can be distinguished by values of RQA (Fig. 6.4, lower part). Particularly, the increase of synchronization between signals, from no interaction to full entrainment, is marked by an increased number of recurrence points and of diagonals in the RPs, which lead

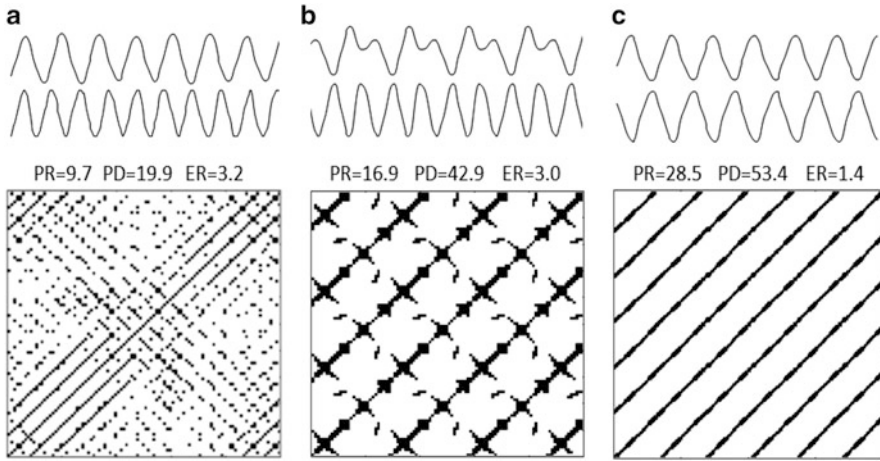


Fig. 6.4 Simulation results obtained with the Van der Pol oscillator. From top to the bottom: the tracks of the oscillator and the forcing term, the RQA results, and the RPs. **A:** no interaction phenomena; **B:** sub-harmonic synchronization; **C:** full entrainment

to increased values of PR and PD. Conversely, ER decreases from no-interaction to full-entrainment. The higher the synchronization between the time series, the more deterministic their interaction, the smaller the ER value. ER is higher when the diagonals have different lengths, regardless the number of the diagonals themselves.

6.4 Cardiorespiratory Synchronization Experiment

The results showed in this chapter refer to an experimental protocol aimed at analyzing the interference between heart rate variability (HRV), blood pressure variability (BPV) and respiration. This protocol was based on the simultaneous acquisition of ECG, Arterial Blood Pressure (ABP) and Respiratory Activity (RA). Surface ECG (II lead) was recorded by an analog electrocardiograph (MCR I, Esaote, Italy). APB was continuously and non-invasively recorded by plethysmographic technique (Finapres, Omheda, USA), and RA was monitored using a pletismographic thoracic belt. The signals were sampled in real-time (sampling frequency: 500 Hz, resolution: 12 bit, DT2801A, Data Translation, USA) and stored for off-line analysis.

We extracted the HRV signal from the low-pass filtered event series (ES) as it is a reliable time domain representation with high temporal resolution. In ES, each beat is replaced by a δ function, and to obtain the HRV series, the ES is low-pass filtered at 0.5 Hz and re-sampled at 2 Hz.

Blood pressure variability (BPV) and the RA series were obtained by a similar low-pass filtering procedure (FIR, 10 order, cut-off frequency 0.5 Hz) and

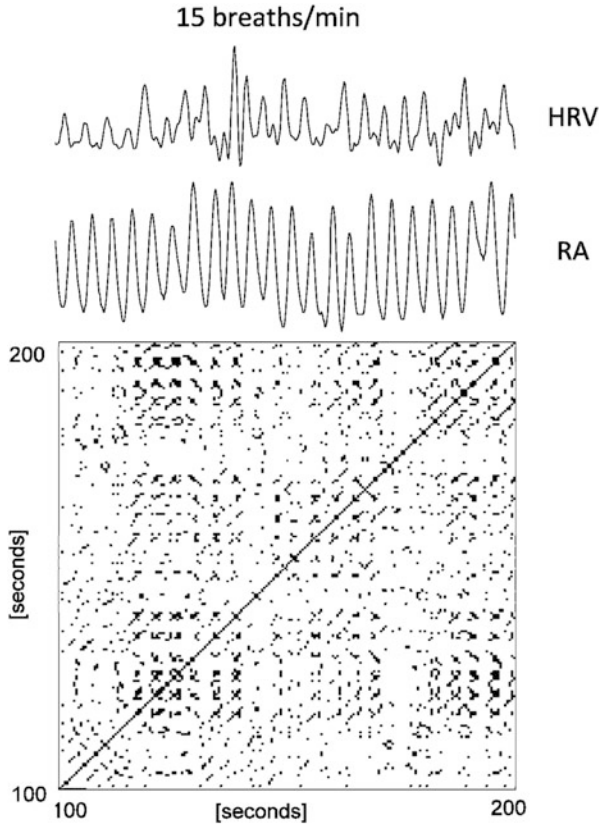


Fig. 6.5 Experimental results obtained during 15 breath/min. 100-second tracks of HRV and respiratory time series are reported, together with the corresponding RP

re-sampling at 2 Hz. According to this procedure, the HRV and RA series were expressed in arbitrary units (a.u., not indicated in the figures), and BPV in mmHg.

The protocol consisted of three stages, with the subject in paced breathing at various rates, lying supine in rest. Each stage lasted 8 min, followed by a 3-min recovery period to allow the periodic calibration of the Finapres. Subjects were instructed to initiate a breath with each tone of a series of auditory cues generated by a computer. Subjects were allowed to adjust their tidal volume to a comfortable level to preserve normal ventilation. Since the acquisitions were performed with the subjects in supine position, subjects were asked to lay on the bed at least 20 min before the acquisition beginning, to adapt themselves to the supine position. In order to avoid movement artifacts, subjects were invited to assume a comfortable position and to avoid muscular movements during the recording.

The selected breathing rates were 15, 12, and 8 breath/min corresponding to 0.25, 0.20 and 0.13 Hz, respectively. These breathing rates allowed to have the High Frequency (HF) component (except for 0.13 Hz) getting progressively closer to the spontaneous Low Frequency (LF) (0.04–0.15 Hz). Figures 6.5, 6.6 and 6.7

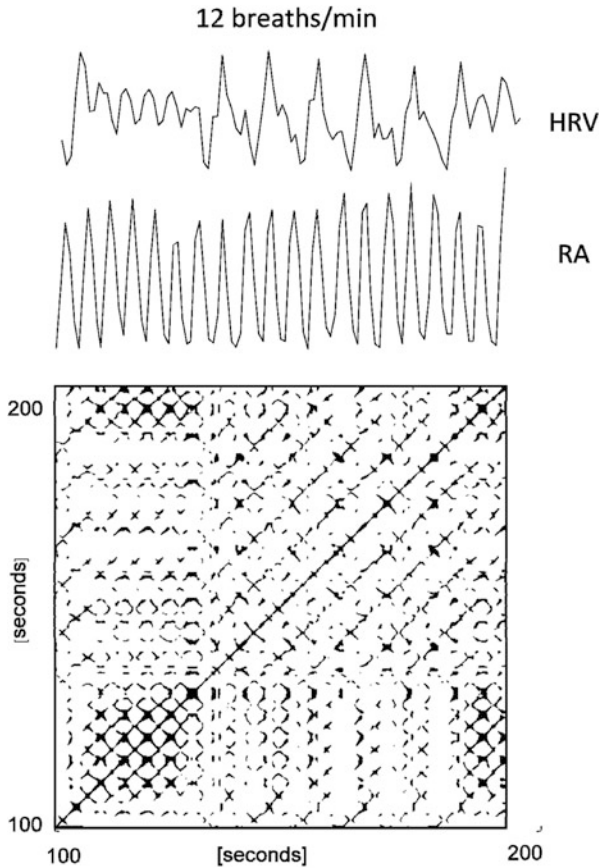


Fig. 6.6 Experimental results obtained during 12 breath/min. 100-second tracks of HRV and respiratory time series are reported, together with the corresponding RP

show the results. 100-second tracks of HRV and respiratory time series are reported, together with the corresponding RP. Note the increase of coupling between the two time series, from 15 to 8 breaths/min stage.

During the 15 breath/min stage the frequency of respiration was 0.25 Hz and the power spectral densities (PSD) of both HRV and BPV signals (not shown) are characterized by an HF component centered at the respiratory frequency and by an LF component which seems not to be influenced by the respiration (center frequency ranging 0.08–0.12 Hz). The RP does not show definite trajectories neither periodicity.

In the 12 breath/min recordings, the interaction between HRV and respiration appeared to have a more complex dynamics. The power spectrum of both HRV showed an LF component clearly centered at half HF frequency (0.10 Hz). Moreover, a more complex, transient interactions between LF and HF components

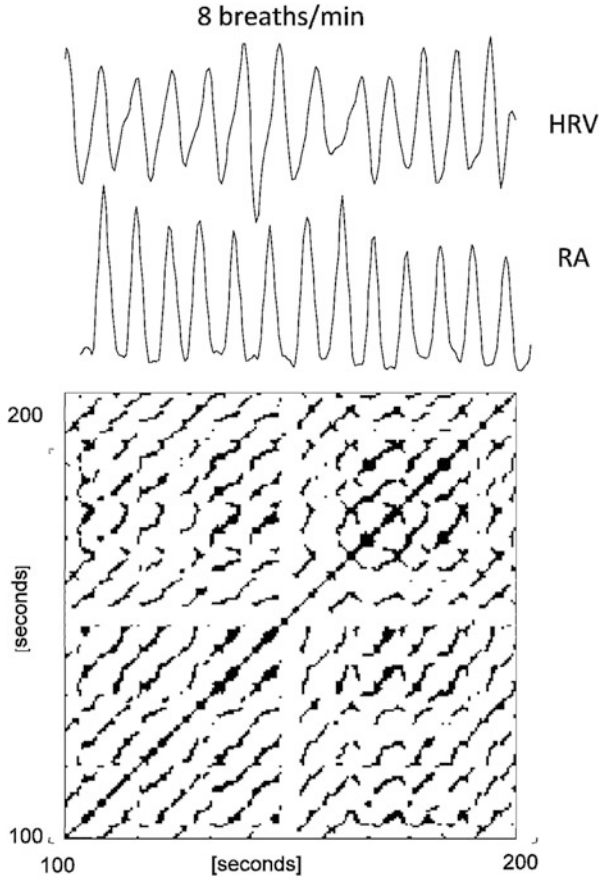


Fig. 6.7 Experimental results obtained during 8 breath/min. 100-second tracks of HRV and respiratory time series are reported, together with the corresponding RP

were observed, which appear to be a 1:2 PL phenomena. This phenomenon appears in the RPs display as diagonal lines recurring every LF period (about 10 s) and isolated points recurring every breath (5 s).

In the 8 breath/min stage only one component (0.13 Hz) and its higher harmonics are visible both in HRV signal: LF and HF components cannot be distinguished anymore and only a unique component centered at the respiratory frequency can be observed and diagonal lines characterize the RP.

Table 6.1 summarizes the results averaged all over the population (mean \pm standard deviation), also reported in Fig. 6.5, panel B.

PR, PD and ER obtained during the 12 breath/min stage are significantly different from those obtained during 15 breath/min stage ($p < 0.001$ for PD and $p < 0.01$ for PR and ER, Wilcoxon's non-parametric test for paired data). PD and PR obtained during 12 breath/min stage are lower than those obtained during 8 breath/min stage,

Table 6.1 RQA results averaged all over the population (mean \pm standard deviation), for the coupling between HRV and respiration

Stage	HRV-respiration		
	PR (mean \pm standard deviation)	PD (mean \pm standard deviation)	ER (mean \pm standard deviation)
15 breath/min	14.8 \pm 4.2	24.5 \pm 4.8	4.2 \pm 0.13
12 breath/min	24.3 \pm 3.5	62.3 \pm 9.2	3.6 \pm 0.2
8 breath/min	27.2 \pm 3.5	68.7 \pm 6.2	2.3 \pm 0.2

whereas ER is higher; in addition the difference of PD and ER values reaches a statistical significance ($p < 0.01$ for PD and $p < 0.001$ for ER). For the three RQA variables, no overlapping is found between 8 and 15 breath/min stages.

6.5 Discussion

We hereby propose a quantitative assessment of the degree of coupling between respiration and cardiovascular variability signals, based on the RQA. We estimated the degree of coupling by quantifying the spatio-temporal recurrent patterns of the interaction between the respiratory rhythm and the HR and BP variability series, in different breathing conditions.

Although the autonomic nervous system (ANS) functionality has been extensively studied by means of spectral and cross-spectral analysis of cardiovascular variability signals, non-linear dynamics have been recently shown to provide a relevant description of operation of this control system [1–8, 31–33]. In addition, the interaction of breathing, heart rate and blood pressure are considered important for the understanding of the functional organization of the ANS.

The ANS functionality has been already investigated by the RQA of single embedded time series of HRV and/or BPV. Dabiré et al. [5] quantified the RP obtained from both HRV and BPV time series by using PR, PD and the longest diagonal, this latter inversely related to the Lyapunov exponent. They showed that these non-linear indexes better reflected the sympathetic tone of BP and the parasympathetic tone of HR, than linear indexes derived from the spectral analysis. The longest diagonal of a RP has been also demonstrated to be a useful index to survey the autonomic function in diabetic subjects. The variability of the cardiovascular signals is very complex and may reflect the non-linear interactions between sympathetic and parasympathetic systems and between the cardiovascular system and the respiratory one. Our approach could provide important physiological information for the understanding of the neurovegetative coordination underlying normal and pathophysiologically disturbed behaviors. Indeed, in normal subjects, the deeper the breaths, the more stretching of the lung, which induces a greater synchronization between lungs and heart both mechanically and neurally.

Obviously, the need to extend the method to a larger number of subjects as well as to the study of pathological situations is crucial. It could be interesting to test whether the non-linear mechanisms and the degrees of non-linear coupling obtained here can be reproduced in more patients, in different experimental conditions, in several patho-physiological conditions of clinical relevance, or in different variability signals (such as microvascular blood flow fluctuations and pupil diameter changes).

RPs have been extensively used to qualitatively detect transient phase locking patterns in the interaction between different oscillators. Following this approach, we used the RQA approach to quantify the repetitive patterns of interaction between respiration and cardiovascular variability signals in a time-to-time domain. An observed recurrent pattern indicates that the (temporal) periodicity of one series has almost the same features as the other series. The number and the length distribution of the diagonals in a RP, measured by PD and ER respectively, encode the deterministic features of the plot itself.

RQA turned out to be suitable for a quantitative evaluation of the observed coupling patterns among rhythms, both in simulated and real data, providing different degrees of coupling. The results from the simulated data showed that the increased degree of coupling between the signals was marked by the increase of PR and PD, and by the decrease of ER. When the RQA was applied to experimental data, PD and ER turned out to be the most significant variables, compared to PR; the better performance of these two variables can be explained by their low intrinsic sensitivity to spurious, isolated recurrent points, which may be introduced by random noise.

Coupling phenomena were investigated during a three-stage paced-breathing protocol, with the respiration rate getting progressively closer to the LF rhythm. Three main results have been obtained: no interaction between LF and HF rhythms at 15 breath/min; transient 1:2 PL phenomena during 12 breath/min stage; 1:1 PL between LF and respiration rhythm during 8 breath/min.

RQA detected different coupling patterns in the three stages of the experimental protocol: no interaction in the first stage (15 breath/min), a kind of sub-harmonic synchronization in the second stage (12 breath/min), and a full entrainment condition in the third one (8 breath/min).

The analysis of the frequency component of the signals by spectral analysis showed that during 15 breath/min the respiratory rhythm did not affect either HRV or BPV spontaneous fluctuations which are characterized by the LF component (but for the respiratory-induced fluctuations). During 12 breath/min, we observed typical sub-harmonic synchronization patterns between the respiration and the cardiovascular variability signals (LF rhythm locked to the half of the respiratory frequency). The LF rhythm resulted to be fully entrained with the respiratory one, during the 8 breath/min stage, in all the subjects examined. However, although the spectral analysis detects shifting of the LF rhythm to the HF frequency all over the recording period, this linear tool considers the cardiovascular variability signal as a linear superposition of oscillations at different frequencies and cannot quantify the degree of non-linear coupling between different rhythms.

The three RQA variables succeeded in discriminating the situation of no-interaction from the full-entrainment, for both the couples HRV-respiration and BPV-respiration. The sub-harmonic synchronization phenomena has been successfully distinguished from the situation of no-interaction but only to a minor extent from that of full synchronization. A certain degree of non-linear coupling exists during the sub-harmonic synchronization phenomenon, significantly higher than that occurring when the LF rhythm seems not to be influenced by the respiratory rhythm. However, the sub-harmonic synchronization is not easily distinguishable from the full-entrainment condition, although generally weaker. It can be speculated that the sub-harmonic synchronization phenomenon is due to a non-linear mechanism somehow similar to that characterizing a full synchronization, but featuring a lower degree of non-linear coupling. Still, it should be noted that ER succeeded in distinguishing between sub-harmonic and full synchronization for both HRV and BPV, while PD did not. This result suggests that the difference between sub-harmonic and full synchronization phenomena can be better detected from the diagonal length distribution (encoded by ER) rather than from the number of diagonals (encoded by PD). Further, since a diagonal length represents the time duration of a recurrence, the two interaction phenomena differ for the duration of stable recurrences and only to a minor extent for their number (quantified by PD). However, the strongest coupling between respiration and cardiovascular variability signals occurs during the last stage of the experimental protocol (8 breaths/min), which elicits a full synchronization between the LF and the HF rhythms in the cardiovascular variability series.

From a physiological viewpoint, it is difficult to precisely identify the mechanisms responsible for the observed non-linear interaction. Our knowledge of the functional organization of the ANS is indeed still incomplete, given its complexity and the large number of involved physiological variables. Several mechanisms can be hypothesized to explain the non-linear coupling between respiratory and spontaneous rhythms of cardiovascular variability signals, such as changes in venous return induced by lung volume, a central coupling of cardiovascular and respiratory centers at the brain stem level, or central non-linear oscillating interacting sources (generating LF, HF and respiratory rhythms) influenced by forcing actions arising from physiologic control loops.

A remarkable finding is the detection of transient 1:2 PL episodes between respiration and cardiovascular variability signals. When the respiration rate was about twice the frequency of the LF rhythm (0.2 Hz, 12 breaths/min stage), the power spectra of HRV and BPV showed a 1:2 frequency relationship between HF and LF rhythms. This phenomenon can be associated to a sub-harmonic synchronization between the two main rhythms of HR and BP variability series, similar to the effect observed in the Van Der Pol model, when the frequency of the external stimulus was about twice the frequency of the self-sustained oscillator. Again, whether this frequency entrainment is stable, or reflects an average behavior cannot be detected by spectral analysis. In four out of eight subjects, the time-domain analysis revealed short-time intervals of stable 1:2 frequency and phase synchronization between RA and HRV. The idea behind the use of the proposed methods is that the

cardiovascular control system features deterministic dynamical properties. This idea is also reflected in the simulated systems used for the verification of the methods. It has to be mentioned that different ideas of the physical nature of the studied signals lead to different mathematical approaches. Analyses based on symbolic dynamics or stochastic modeling might also be used to investigate cardiorespiratory synchronization data.

It can be speculated that phenomena such as 1:2 PL between LF and HF rhythms might be expression of a fine regulation of the ANS. Such synchronization phenomena can be evoked in experimental conditions (control breathing at 12 breaths/min) easily reproducible in clinical practice. In addition, the transient nature of the interaction phenomena could explain the observed amount of non-linear coupling.

Several factors such as the mean heart rate, the spontaneous LF frequency, the overall autonomic balance, and the actual respiration frequency jitter may produce the inter-individual variability observed in the 1:2 PL phenomena. Further investigation of this important point requires a larger number of subjects as well as the quantification of the ‘degree of coupling’ between LF and respiratory rhythms.

References

1. V. Sharma, Deterministic chaos and fractal complexity in the dynamics of cardiovascular behavior: perspectives on a new frontier. *Open Cardiovasc. Med. J.* **3**, 110–123 (2009)
2. D. Hoyer, R. Bauer, B. Walter, U. Zwiener, Estimation of nonlinear couplings on the basis of complexity and predictability – a new method applied to cardiorespiratory coordination. *IEEE Trans. Biomed. Eng.* **45**(5), 545–552 (1998)
3. D. Hoyer, O. Hoyer, U. Zwiener, A new approach to uncover dynamic phase coordination and synchronization. *IEEE Trans. Biomed. Eng.* **47**(1), 68–74 (2000)
4. H. Ding, S. Crozier, S. Wilson, A new heart rate variability analysis method by means of quantifying the variation of nonlinear dynamic patterns. *IEEE Trans. Biomed. Eng.* **54**(9), 1590–1597 (2007)
5. H. Dabiré, D. Mestivier, J. Jarnet, M.E. Safar, N.P. Chau, Quantification of sympathetic and parasympathetic tones by non-linear indexes in normotensive rats. *Am. J. Physiol.* **275**(4 Pt 2), H1290–H1297 (1998)
6. B. Pompe, P. Blindh, D. Hoyer, M. Eiselt, Using mutual information to measure coupling in the cardiorespiratory system. *IEEE Eng. Med. Biol.* **17**(6), 32–39 (1998)
7. J.S. Chang, K. Ha, I.Y. Yoon, C.S. Yoo, S.H. Yi, J.Y. Her, T.H. Ha, T. Park, Patterns of cardiorespiratory coordination in young women with recurrent major depressive disorder treated with escitalopram or venlafaxine. *Prog. Neuropsychopharmacol. Biol. Psychiatry* **39**(1), 136–142 (2012)
8. E. Pereda, D.M. De la Cruz, L. De Vera, J.J. González, Comparing generalized and phase synchronization in cardiovascular and cardiorespiratory signals. *IEEE Trans. Biomed. Eng.* **52**(4), 578–583 (2005)
9. J.P. Eckmann, S.O. Kamphorst, D. Ruelle, Recurrence plots of dynamical systems. *Europhys. Lett.* **4**, 973–977 (1987)
10. C.L. Webber, J.P. Zbilut, Dynamical assessment of physiological systems and states using recurrence plot strategies. *J. Appl. Physiol.* **76**(2), 965–973 (1994)

11. S. Ramdani, G. Tallon, P.L. Bernard, H. Blain, Recurrence quantification analysis of human postural fluctuations in older fallers and non-fallers. *Ann. Biomed. Eng.* **41**, 1713–1725 (2013)
12. C.D. Nguyen, S.J. Wilson, S. Crozier, Automated quantification of the synchrogram by recurrence plot analysis. *IEEE Trans. Biomed. Eng.* **59**(4), 946–955 (2012)
13. M. Mohebbi, H. Ghassemian, Prediction of paroxysmal atrial fibrillation using recurrence plot-based features of the RR-interval signal. *Physiol. Meas.* **32**(8), 1147–1162 (2011)
14. U.R. Acharya, S.V. Sree, S. Chattopadhyay, W. Yu, P.C. Ang, Application of recurrence quantification analysis for the automated identification of epileptic EEG signals. *Int. J. Neural Syst.* **21**(3), 199–211 (2011)
15. Y. Peng, Z. Sun, Characterization of QT and RR interval series during acute myocardial ischemia by means of recurrence quantification analysis. *Med. Biol. Eng. Comput.* **49**(1), 25–31 (2011)
16. M. Mazaheri, H. Negahban, M. Salavati, M.A. Sanjari, M. Parnianpour, Reliability of recurrence quantification analysis measures of the center of pressure during standing in individuals with musculoskeletal disorders. *Med. Eng. Phys.* **32**(7), 808–812 (2010)
17. P.I. Terrill, S.J. Wilson, S. Suresh, D.M. Cooper, C. Dakin, Attractor structure discriminates sleep states: recurrence plot analysis applied to infant breathing patterns. *IEEE Trans. Biomed. Eng.* **57**(5), 1108–1116 (2010)
18. S. Raiesdana, S.M. Golpayegani, S.M. Firoozabadi, J. Mehvari Habibabadi, On the discrimination of patho-physiological states in epilepsy by means of dynamical measures. *Comput. Biol. Med.* **39**(12), 1073–1082 (2009)
19. A. Porta, G. Baselli, N. Montano, T. Gneccchi-Ruscone, F. Lombardi, A. Malliani, S. Cerutti, Non-linear dynamics in the beat-to-beat variability of sympathetic activity in decerebrate cats. *Methods Inf. Med.* **33**, 89–93 (1994)
20. N. Marwan, J. Kurths, Nonlinear analysis of bivariate data with cross recurrence plots. *Phys. Lett. A* **302**, 299–307 (2002)
21. M. Carmen Romano, M. Thiel, J. Kurths, W. von Bloh, Multivariate recurrence plots. *Phys. Lett. A* **330**, 214–223 (2004)
22. A. Porta, G. Baselli, N. Montano, T. Gneccchi-Ruscone, F. Lombardi, A. Malliani, S. Cerutti, Classification of coupling patterns among spontaneous rhythms and ventilation in the sympathetic discharge of decerebrated cats. *Biol. Cybern.* **75**, 163–172 (1996)
23. F. Censi, V. Barbaro, P. Bartolini, G. Calcagnini, A. Michelucci, G.F. Gensini, S. Cerutti, Spatio-temporal recurrent patterns of atrial depolarization during atrial fibrillation assessed by recurrence plot quantification. *Ann. Biomed. Eng.* **28**(1), 61–70 (2000)
24. H. Ando, H. Suetani, J. Kurths, K. Aihara, Chaotic phase synchronization in bursting-neuron models driven by a weak periodic force. *Phys. Rev. E Stat. Nonlin. Soft Matter Phys.* **86**(1 Pt 2), 016205.25 (2012)
25. M.C. Mackey, L. Glass, Oscillation and chaos in physiological control systems. *Science* **197**, 287–289 (1977)
26. M.R. Guevara, L. Glass, A. Shrier, Phase locking, period-doubling bifurcations, and irregular dynamics in periodically stimulated cardiac cells. *Science* **214**, 1350–1352 (1981)
27. S.D. Wu, P.C. Lo, Cardiorespiratory phase synchronization during normal rest and inward-attention meditation. *Int. J. Cardiol.* **141**(3), 325–328 (2010)
28. M.C. Wu, C.K. Hu, Empirical mode decomposition and synchrogram approach to cardiorespiratory synchronization. *Phys. Rev. E Stat. Nonlin. Soft Matter Phys.* **73**(5 Pt 1), 051917 (2006)
29. V. Perltz, B. Cotuk, M. Lambertz, R. Grebe, G. Schiepek, E.R. Petzold, H. Schmid-Schönbein, G. Flatten, Coordination dynamics of circulatory and respiratory rhythms during psychomotor drive reduction. *Auton. Neurosci.* **115**(1–2), 82–93 (2004)
30. M.D. Prokhorov, V.I. Ponomarenko, V.I. Gridnev, M.B. Bodrov, A.B. Bespyatov, Synchronization between main rhythmic processes in the human cardiovascular system. *Phys. Rev. E Stat. Nonlin. Soft Matter Phys.* **68**(4 Pt 1), 041913 (2003)
31. G.M. Ramírez Ávila, A. Gapelyuk, N. Marwan, H. Stepan, J. Kurths, T. Walther, N. Wessel, Classifying healthy women and preeclamptic patients from cardiovascular data using recurrence and complex network methods. *Auton. Neurosci.* **178**, 103–110 (2013)

32. R. Guo, Y. Wang, J. Yan, H. Yan, Recurrence quantification analysis on pulse morphological changes in patients with coronary heart disease. *J. Tradit. Chin. Med.* **32**(4), 571–577 (2012)
33. M. Javorka, Z. Turianikova, I. Tonhajzerova, K. Javorka, M. Baumert, The effect of orthostasis on recurrence quantification analysis of heart rate and blood pressure dynamics. *Physiol. Meas.* **30**(1), 29–41 (2009)